Multi-Scale MHD Analysis Incorporating Pressure Transport Equation for Beta-Increasing LHD Plasma

K. Ichiguchi 1), B. A. Carreras 2)

1) National Institute for Fusion Science, Oroshi-cho 322-6, Toki, Gifu, 509-5292, Japan
2) BACV Solutions Inc., 110 Mohawk, Oak Ridge, Tennessee 37831, USA

e-mail contact of main author: ichiguch@nifs.ac.jp

Abstract. A multi-scale MHD numerical scheme is developed for the analysis of nonlinear evolution of beta-increasing plasma. The scheme is based on the iterative calculations of nonlinear dynamics based on the reduced MHD (RMHD) equations and three-dimensional static equilibrium. The equation for average pressure in the RMHD equation plays a roll of a transport equation that involves a heat source term and background pressure diffusion term. The heat source term is controlled so that the beta value should be increased in a constant rate. The scheme is applied to a configuration of the Large Helical Device (LHD), where ideal interchange modes are predicted to be unstable while beta values much higher than the predicted limit are obtained in the experiments. Local flat structure is generated in the background pressure profile due to the nonlinear saturation of the interchange modes. The generation reduces the driving force of the modes at higher beta value. Such self-organization in the pressure profile is considered to be the stabilizing mechanism in the plasma.

1. Introduction

In experiments in the LHD, high beta plasmas have been successfully obtained. Particularly, average beta of $\langle\beta\rangle = 5\%$ was achieved in the inward-shifted configuration with the vacuum magnetic axis located at $R_{ax} = 3.6$m[1]. On the other hand, in this configuration, equilibria calculated under the assumption of a parabolic pressure profile that is close to the profile observed in the experiments are predicted to be unstable against linear ideal interchange modes at much lower beta values than 5%[2]. The result indicates existence of a stabilizing mechanism that cannot be explained by the linear ideal stability theory. We investigate the mechanism in the point of nonlinear evolution of the plasma by utilizing a nonlinear dynamics code called NORM[3], which is based on the RMHD equations.

Since the interchange mode is a pressure driven mode, the stability property strongly depends on the beta value through the change of the equilibrium. Therefore, for the consistent study of the mechanism, it is necessary to incorporate beta increase effect for equilibrium quantities as well as perturbations in the analysis. However, there is a big difference in the time scales between the equilibrium evolution and the perturbation dynamics, which is in the order of 10^5 - 10^6. To analyze this multi-scale problem, we develop an iterative scheme with the NORM code and the VMEC equilibrium code[4]. In the original scheme[5,6], the equilibrium is updated every short time interval of the dynamics calculation of the perturbations. The beta value is increased stepwise by adding a small increment to the background pressure when the equilibrium is updated. By applying this scheme to the low beta LHD plasma we observed self-organization of the pressure profile[5,6].

The scheme has been significantly extended so that continuous heating and diffusion of the background pressure can be taken into account[7]. In this scheme, the equation for the average

pressure is separately treated as a pressure transport equation. The beta value is increased by means of the heat source term in the equation. In Ref.[7], we obtained a preliminary result for the LHD plasma by using a fixed heat source. In this case, the beta value is saturated at a low level in the time evolution due to the diffusion of the background pressure. Thus, in the present work, we control the heat source term so that the beta value can be increased in a constant rate. This control makes it possible to avoid the saturation of the beta and to examine the plasma behavior up to any high beta value in principle. We apply the scheme to the LHD plasma to investigate the stabilizing mechanism.

2. Multi-Scale Scheme Incorporating Pressure Transport Equation

Here we review the multi-scale scheme incorporating a pressure transport equation briefly and explain how the heat source term is controlled in the present analysis. The nonlinear dynamics calculation in the scheme is based on the RMHD equations for poloidal flux Ψ, stream function Φ and pressure P[3]. Here, we separate the variables differently. The poloidal flux and the stream function are separated into equilibrium and perturbed parts as

$$\Psi(\rho,\theta,\zeta;t) = \Psi_{eq}(\rho) + \tilde{\Psi}(\rho,\theta,\zeta;t) \quad \text{and} \quad \Phi(\rho,\theta,\zeta;t) = \tilde{\Phi}(\rho,\theta,\zeta;t), \tag{1}$$

respectively, while the pressure is separated into average and oscillating parts,

$$P(\rho,\theta,\zeta;t) = \langle P\rangle(\rho;t) + \widehat{P}(\rho,\theta,\zeta;t). \tag{2}$$

Here we employ the flux coordinates (ρ,θ,ζ), where ρ denotes the square root of the normalized toroidal magnetic flux, and θ and ζ are the poloidal and the toroidal angles, respectively. The subscript '*eq*' and the tilde indicate the equilibrium and the perturbed quantities, respectively. The angle bracket and the hat indicate the average and the oscillating parts, respectively. By substituting these separated variables into the RMHD equations, we obtain the equations for $\tilde{\Psi}$, $\tilde{\Phi}$, $\widehat{P}$ and $\langle P\rangle$, which are given by

$$\frac{\partial\tilde{\Psi}}{\partial t} = -\nabla_{\parallel}\tilde{\Phi} + \frac{1}{S}\tilde{J}_{\zeta}, \tag{3}$$

$$\frac{\partial\tilde{U}}{\partial t} = -[\tilde{U},\tilde{\Phi}] - \nabla_{\parallel}\tilde{J}_{\zeta} - [\tilde{\Psi},J_{\zeta eq}] + \frac{1}{2\varepsilon^2}[\Omega_{eq},\widehat{P}] + \nu\left(\frac{R}{R_0}\right)^2\nabla_{\perp}^2\tilde{U}, \tag{4}$$

$$\frac{\partial\widehat{P}}{\partial t} = -\widehat{[P,\tilde{\Phi}]} + \kappa_{\perp}\widehat{\Delta_* P} + \kappa_{\parallel}\widehat{\nabla_{\parallel}^{\dagger 2}P} \tag{5}$$

and

$$\frac{\partial\langle P\rangle}{\partial t} = -\langle[\widehat{P},\tilde{\Phi}]\rangle + \kappa_{\perp}\langle\Delta_*\langle P\rangle\rangle + \kappa_{\parallel}\langle\nabla_{\parallel}^{\dagger 2}\langle P\rangle\rangle + Q. \tag{6}$$

Here $[y,z]$ denotes the Poisson bracket which is defined as $[y,z] = (g/\rho)((\partial y/\partial\rho)(\partial z/\partial\theta) - (\partial y/\partial\theta)(\partial z/\partial\rho))$. The diffusion operators Δ_* and $\nabla_{\parallel}^{\dagger 2}$ are defined as $\Delta_* f = \left(R/R_0^2\right)^2\nabla_{\perp}\cdot\left(R/R_0^2\right)^2\nabla_{\perp} f$ and $\nabla_{\parallel}^{\dagger 2} f = \nabla_{\parallel}\left[\left(R/R_0^2\right)^2\nabla_{\parallel} f\right]$, respectively, where R/R_0 denotes the normalized major radius. The perpendicular and the parallel differential operators are given by $\nabla_{\perp} f = \nabla f - \nabla\zeta(\partial f/\partial\zeta)$ and $\nabla_{\parallel} f = g(\partial f/\partial\zeta) + [\Psi, f]$, respectively, where g is a factor corresponding to diamagnetic effect. The current density and the vorticity in the toroidal direction are given by

$J_\zeta = \Delta_* \Psi$ and $U = (R/R_0)^2 \nabla_\perp^2 \Phi$, respectively. Factors of ε, S, ν, $\kappa_\perp$ and $\kappa_\parallel$ are inverse aspect ratio, magnetic Reynolds number, viscosity coefficient and heat conductivities perpendicular and parallel to the magnetic field, respectively, and Ω_{eq} denotes the average field line curvature. In the present analysis, the values of $S = 1.0 \times 10^6$, $\nu = 1.7 \times 10^{-4}$ $\kappa_\perp = 1.7 \times 10^{-6}$ and $\kappa_\parallel = 1.7 \times 10^{-2}$ are assumed. A heat source term Q is added in eq.(6), which is utilized for the increase of beta.

In this formulation, we treat $\langle P \rangle$ as the background equilibrium pressure. The pressure can be changed by both the finite beta value and the perturbation dynamics. Equation (6) expresses the dynamics of the background pressure. The equation consists of the convection, the perpendicular and the parallel diffusion of the average pressure and the heat source term. These terms correspond to the anomalous diffusion due to the nonlinear turbulence, the classical heat diffusion and the continuous heating, respectively. Thus, the equation plays a role of a transport equation in the scheme.

The scheme consists of a series of time evolution steps for a certain time interval. The time evolution in each interval is calculated with a predictor-corrector method. Here we consider to increase the average beta value from $\langle \beta \rangle_i$ to $\langle \beta \rangle_{i+1}$ in the interval of $t_i \le t \le t_{i+1}$. In the predictor step, the equilibrium pressure P_{eq}^{pre} is calculated at the beginning ($t = t_i$) and the end ($t = t_{i+1}$) of the interval at first. For the equilibrium pressure at $t = t_i$, the calculation result for $\langle P \rangle$ in the interval of $t_{i-1} \le t \le t_i$ is employed, i.e., $P_{eq,i}^{pre} = \langle P \rangle_i$. The equilibrium pressure at $t = t_{i+1}$ is calculated by the addition of an increment pressure as,

$$P_{eq,i+1}^{pre} = \langle P \rangle_i + \Delta P_{i+1}^{pre}(\rho). \tag{7}$$

Here ΔP_{i+1}^{pre} is an increment of the pressure, which is given by

$$\Delta P_{i+1}^{pre}(\rho) = (\langle \beta \rangle_{i+1} - \langle \beta \rangle_i) F_P(\rho), \tag{8}$$

where $F_P(\rho)$ is a given profile. The equilibria at $t = t_i$ and $t = t_{i+1}$ are calculated by means of the VMEC code for $P_{eq,i}^{pre}$ and $P_{eq,i+1}^{pre}$, respectively. By interpolating the equilibrium quantities at $t = t_i$ and t_{i+1}, we obtain the quantities at every time step of the dynamics calculation with the NORM code. The heat source term in eq.(6) is determined so as to be consistent with the pressure increment as

$$Q_{i+1}^{pre} = \frac{\Delta P_{i+1}^{pre}}{t_{i+1} - t_i} \tag{9}$$

Then, we follow the time evolution of the dynamics by means of the NORM code with the interpolated equilibrium quantities and the heat source.

In the corrector step, the result of the dynamics calculation in the predictor step $\langle P \rangle_{i+1}^{pre}$ is utilized in the calculation of the equilibrium pressure at $t = t_{i+1}$. In this case, the reduction of the pressure due to the diffusion have to be compensated. The equilibrium pressure is given by

$$P_{eq,i+1}^{cor} = \frac{\langle \beta \rangle_{i+1}}{\langle \beta \rangle_{i+1}^{pre}} \langle P \rangle_{i+1}^{pre}, \tag{10}$$

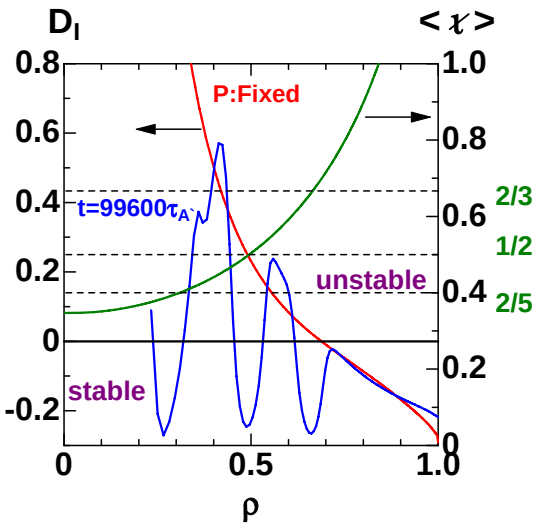

FIG.1. Profiles of D_I for the cases of the fixed equilibrium pressure profile at $\langle\beta\rangle = 0.716\%$ of $P = P_0(1-\rho^2)(1-\rho^8)$ (red line) and the beta increasing scheme at $\langle\beta\rangle = 0.713\%$ (blue line). Positive and negative values indicate stable and unstable regions, respectively. Profile of the rotational transform in the equilibrium for $P = P_0(1-\rho^2)(1-\rho^8)$ is also plotted.

where $\langle\beta\rangle_{i+1}^{pre}$ is the average beta value obtained at $t = t_{i+1}$ in the predictor calculation corresponding to $\langle P\rangle_{i+1}^{pre}$. The pressure increment for the heat source term is evaluated as,

$$\Delta P_{i+1}^{cor} = \left[\frac{(\langle\beta\rangle_{i+1})^2}{\langle\beta\rangle_{i+1}^{pre}} - \langle\beta\rangle_i\right] F_P(\rho). \tag{11}$$

As in the case of the predictor step, the heat source term in eq.(6) is determined as

$$Q_{i+1}^{cor} = \frac{\Delta P_{i+1}^{cor}}{t_{i+1}-t_i} = Q_{0,i+1} F_P(\rho). \tag{12}$$

Then, the dynamics is calculated again with the NORM code for the corrector step. In the present work for the LHD plasma, we employ a constant increasing rate of the beta value. Hence, we use ΔP_i^{cor} for ΔP_{i+1}^{pre} instead of eq.(8) to enhance the accuracy in the predictor step.

3. Magnetic Configuration and Nonlinear Dynamics for a Fixed Equilibrium Pressure

In the present work, we investigate the stabilizing mechanism of the LHD plasma in the configuration with the vacuum magnetic axis located at $R_{ax} = 3.6$m. In the vacuum configuration, the rotational transform increases monotonously in the range of $0.35 \leq \iota \leq 1.8$. Before studying the beta-increasing case with the multi-scale scheme, we examine the nonlinear behavior of the plasma for a fixed equilibrium pressure for the comparison. We employ a currentless equilibria at $\langle\beta\rangle = 0.716\%$ with a parabolic pressure profile of

$$P_{eq} = P_0(1-\rho^2)(1-\rho^8). \tag{13}$$

This profile is close to the observed one in the experiments at low beta[8]. This equilibrium is unstable against linear interchange modes. The core region of $\rho \leq 0.689$ is Mercier unstable

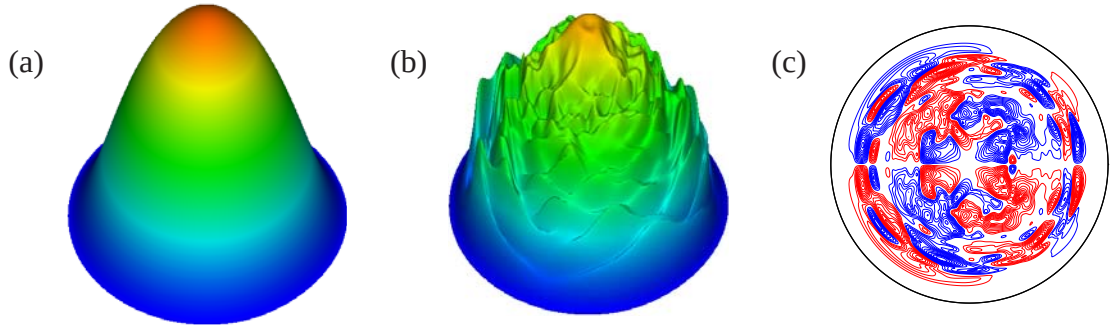

FIG.2. Bird's eye view of total pressure for the fixed equilibrium pressure at (a) $t = 0\tau_A$, (b) $t = 4490\tau_A$, and (c) stream lines at $t = 3630\tau_A$.

as shown in Fig.1. The absolute value of the Mercier quantity D_I[9] has a very large value at the rational surfaces of $\iota = 2/5$, 1/2 and 2/3. The property of D_I indicates that multiple global modes with low mode numbers have significant growth rates.

We follow the time evolution of the nonlinear dynamics for the fixed equilibrium pressure. Figure 2 (a) and (b) are the total pressure at $t = 0\tau_A$ and $4490\tau_A$, where τ_A denotes Alfvén time. The pressure collapses in a short time as shown in Fig.2(b). In the time evolution, several global modes with different mode numbers grow simultaneously at different rational surfaces. In the early stage, each mode is localized around its resonant surface. As the modes grow, the radial width of the vortices becomes wider. Then, the vortices of the modes overlap and merge each other. As a result, large vortices are generated as shown in Fig.2 (c). The vortices convect the pressure from the core to the edge and lead to the rapid collapse. This situation corresponds to a minor disruption. However, this is not the case of the LHD plasma. The plasmas at much higher beta value are obtained without such disruptive phenomena in the experiments.

4. Multi-Scale Analysis of Beta Increasing Plasma

Next, we apply the multi-scale numerical scheme to the LHD plasma. The average beta value is increased from $\langle\beta\rangle = 0.220\%$ to 1.054% in a constant rate. The increasing rate is controlled so as to be $0.5 \times 10^{-5}\%/\tau_A$ as shown in Fig.3. We use the profile of $F_P = (1-\rho^2)(1-\rho^8)$ for the initial pressure profile as well as the profile of the heat source term given by eq.(12). Then, the factor Q_0 is increased as the average beta value is increased, as shown in Fig.3.

Figure 3 also shows the time evolution of the total kinetic energy. As the beta value is increased in time, interchange modes are excited. However, we do not observe any disruptive phenomena in the time evolution. A smooth evolution of the axis beta value β_0 also indicates no disruptive event in the core region. Note that the beta value is increased beyond the value at which a disruptive phenomenon occurs for the fixed equilibrium pressure. In the beta increasing case, low-n modes are excited and saturated successively. The $(m,n) = (5,2)$, (4,2) and (3,2) modes are excited at $t \simeq 10800\tau_A$, $24000\tau_A$ and $72000\tau_A$, respectively, where m and n are the poloidal and the toroidal mode numbers. This is due to the property of D_I profile. The profile of D_I at $\langle\beta\rangle = 0.220\%$ is a monotonous decreasing function of ρ as that of $\langle\beta\rangle = 0.716\%$ shown in Fig.1. Therefore, modes resonant in the core region are excited at lower beta value than those in

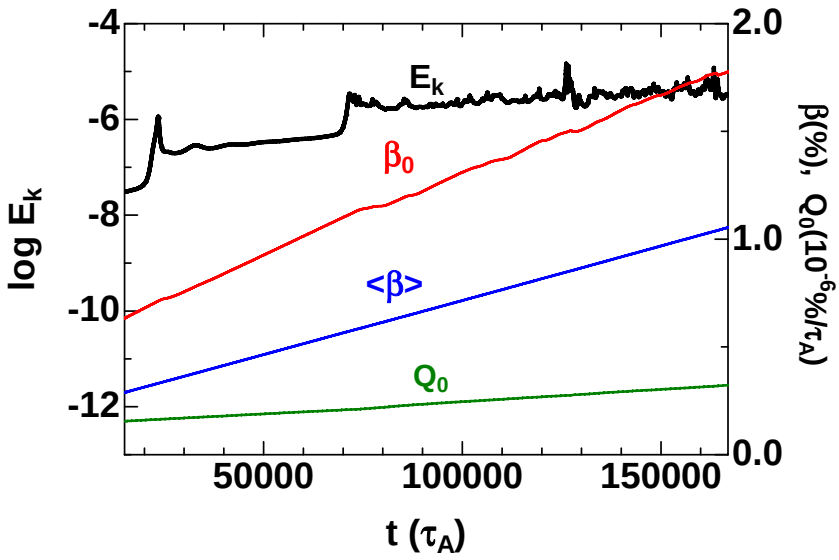

FIG.3. Time Evolution of kinetic energy E_k, axis beta value β_0, average beta value $\langle\beta\rangle$ and amount of heat source term Q_0 normalized by magnetic pressure and Alfvén time.

edge region. As the beta value is increased, each mode is excited just after the pressure gradient at the resonant surface exceeds the marginal value. Therefore, the driving force is small when the mode is excited. Thus, even the mode is excited, the excitation is weak and saturation occurs immediately.

Since the mode excitation is weak, deformation of the pressure profile due to the modes is limited around the resonant surfaces. This situation is seen in the time evolution of the total pressure and the stream lines, which are shown in Fig.4. The total pressure varies depending on the excitation of the modes. However, the structure with the mode number is almost retained around each resonant surface. This means that each mode is localized around its resonant surface. The localization of each mode is confirmed in the patterns of the stream lines. The vortices are localized around the resonant surfaces and they do not overlap each other. Figure 4(b) shows the pressure and the stream lines at almost the same beta value as in Fig.2. Comparison of the results indicates that the localization of the modes avoids the disruptive phenomenon.

Even after the mode saturation, the beta value is still increased, and therefore, the driving force should be enhanced. Nevertheless, the mode-overlapping which causes a disruptive phenomenon is suppressed in the time evolution. The suppression is attributed to the deformation of the background pressure profile. As shown in Fig.5, the weak excitation of a mode generate local flat structure around the resonant surface in the profile. Such structure decreases the driving force of the mode and reduces the growth at higher beta. Therefore, the local reduction of the background pressure gradient due to the nonlinear dynamics is considered to be the stabilizing mechanism of the LHD plasma. The stabilizing effect is directly seen in the linear stability. Figure 1 shows the profile of the Mercier quantity D_I at $\langle\beta\rangle = 0.713\%$ and $t = 99600\tau_A$. The Mercier stability is locally improved around the resonant surfaces of $\iota = 2/5$, 1/2 and 2/3, where the local flat structure is generated as shown in Fig.5. Thus, the pressure profile is self-

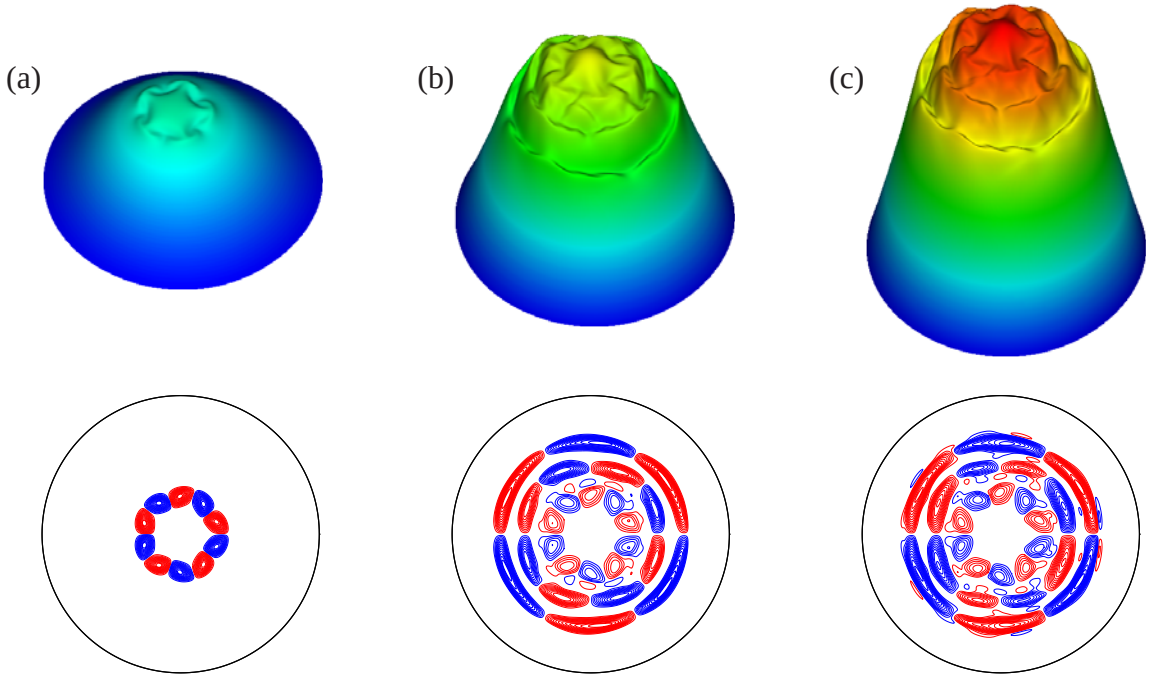

FIG.4. Bird's eye view of total pressure and stream lines at (a) $t = 10800\tau_A$ *(*$\langle\beta\rangle = 0.268\%$*), (b)* $99600\tau_A$ *(*$\langle\beta\rangle = 0.713\%$*) and (c)* $166800\tau_A$*(*$\langle\beta\rangle = 1.054\%$*).*

organized continuously in the beta increasing LHD plasma so that disruptive phenomena should be suppressed.

The pressure transport equation involves a term describing a convection due to the nonlinear dynamics, which corresponds to anomalous diffusion due to the interchange modes. Thus, we also evaluate the convective transport. Figure 6 shows the time evolutions of the average pressure flux $\langle\widehat{P}\tilde{v}^{\rho}\rangle$ corresponding to the term. The flux is enhanced at the local flat regions in the background pressure profile. This result implies that the convection due to the interchange modes remains to keep the flat structure in the pressure profile. Therefore, from transport time scales the pressure evolution can be interpreted as a diffusion process with a diffusion coefficient with a radial structure like the one shown by the flux in Fig.6.

5. Concluding Remarks

By developing a multi-scale MHD scheme for the analysis of beta-increasing plasma, we obtain that the beta value of the LHD plasma unstable to linear ideal interchange modes can be increased beyond the value at which a disruptive phenomenon occurs for a fixed equilibrium pressure profile. The stabilizing mechanism is the reduction of the driving force due to the generation of local flat structure in the background pressure profile. The local flat structure is successively generated at different rational surfaces by the saturation of the weakly excited modes. As a result, vorticity overlapping is avoided and disruptive phenomenon is suppressed. Such self-organization can be revealed only in the analysis with the scheme including the beta-increasing effect.

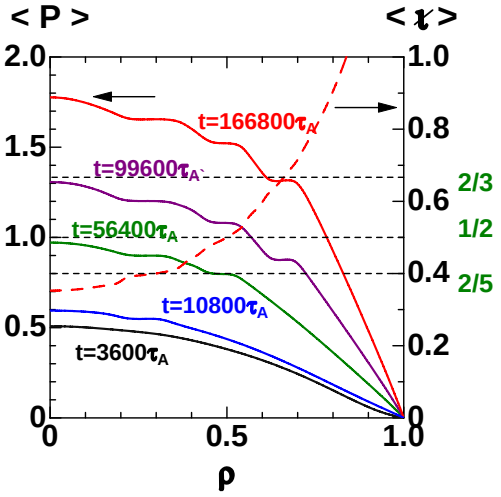

FIG.5. Profiles of background pressure at $t = 3600\tau_A$, $t = 10800\tau_A$, $t = 56400\tau_A$, $t = 99600\tau_A$ and $t = 166800\tau_A$, and rotational transform at $t = 166800\tau_A$.

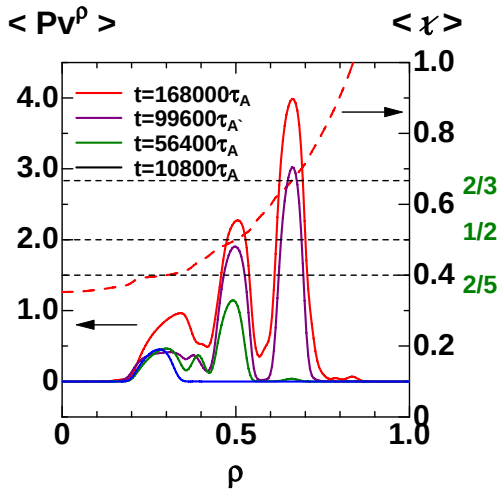

FIG.6. Profiles of $\langle \widehat{\tilde{P}\tilde{v}^{\rho}} \rangle$ at $t = 3600\tau_A$, $t = 10800\tau_A$, $t = 56400\tau_A$, $t = 99600\tau_A$ and $t = 166800\tau_A$, and rotational transform at $t = 166800\tau_A$.

The deformation of the pressure profile is not a simple superposition of each local quasi-linear change. The generation of a flat region enhances the gradient in the vicinity. The enhancement has a destabilizing contribution to the mode resonant at the region. Therefore, there are interactions between multiple modes with different helicities through the change of the pressure gradient. Furthermore, both the continuous heating and the background pressure diffusion have an effect to smooth out the local flat structure and also influence the interaction between the modes. Under the situation, the plasma is continuously self-organized as the beta increases so that the vortices of all of the modes should not overlap as a whole. The result obtained here indicates the existence of a stable path to a high beta regime obtained in the experiments.

Acknowledgment

This work is partly supported by a budget NIFS10KLDT005 of the National Institute for Fusion Science, and Grant-in-Aid for Scientific Research (C) 22560822 of JSPS Japan.

References

[1] KOMORI, A., et al., “Development of Net-Current Free Heliotron Plasmas in the Large Helical Device”, Proc. 22nd Fusion Energy Conf. Oct.13-18, 2008, Geneva, OV/2-4.
[2] ICHIGUCHI, K., “Ideal and Resistive Stability of Free-Boundary LHD Equilibria”, Proc. 1999 Intl. Stellarator Workshop, Madison, 1999, CD-ROM file P2-4 (2000).
[3] ICHIGUCHI, K., et al., Nucl. Fusion **43** (2003) 1101.
[4] HIRSHMAN, S.P., et al., Comp. Phys. Comm. **43** (1986) 143.
[5] ICHIGUCHI, K., CARRERAS, B. A., J. Plasma Phys. **72** (2006) 1117.
[6] ICHIGUCHI, K., CARRERAS, B. A., Plasma and Fusion Res., **3** (2008) S1033.
[7] ICHIGUCHI, K., CARRERAS, B. A., J. Plasma Fusion Res. SERIES **8** (2009) 1171.
[8] LIANG, Y., et al., Plasma Phys. Control. Fusion **44** (2002) 1383.
[9] JOHNSON, J.L., and GREEN, J.M., Plasma Phys. **9** (1967) 611.